

# Electron Cyclotron Radiation Studies Using the ASTRA Transport Code Coupled with the CYTRAN Routine

DIES Javier, GARCÍA Jerónimo, ALBAJAR Ferran, FONTDECABA Josep Maria,  
CORTÉS Guillem and IZQUIERDO Jesús

*Fusion Energy Engineering Laboratory (FEEL), Departament de Física i Enginyeria Nuclear,  
ETSEIB, Universitat Politècnica de Catalunya (UPC), Barcelona (Spain)*

(Received: 9 December 2003 / Accepted: 14 May 2004)

## Abstract

The non-local effects of the EC radiative transfer on the electron temperature profile are analyzed for high-temperature plasmas as those expected in non-inductive ITER scenarios. For this purpose a 1D transport code has been coupled with a model for the EC radiative power density, and the sensitivity of the electron temperature to the wall-reflectivity has been evaluated. The results obtained by letting the temperature as a free parameter show a broadening of the temperature radial profile when the non-local model is considered. Moreover, the temperature resulting of the steady-state plasma equilibrium is shown to be strongly sensitive to the wall reflectivity.

## Keywords:

Electron Clyclotron, advanced scenarios, ITER, energy transport

## 1. Introduction

While Electron Cyclotron radiation losses are weak in present-day magnetically confined plasmas, these effects may become important in next step devices, mainly due to their strong dependence on plasma electron temperature ( $T_e$ ), approximated by,  $P_{cyc} \propto Te^{5/2}$ .

In 1D transport studies, the calculation of the Electron Cyclotron (EC) power loss is generally performed using locally applied global models [1,2]. However, it was shown [3,4] that a more accurate analysis is required owing to the non-local nature of the radiation transport for the dominant part of EC emission spectrum at the high temperatures envisaged for plasmas of fusion interest [5]. These studies also reveal that in the outer part of the plasma net EC power absorption rather than emission may occur if the reflectivity of the wall is sufficiently high. Furthermore it is known that for ITER-like plasma conditions [6], at high electron temperature as expected in the so-called “advanced” transport regimes, EC losses tend to be larger than bremsstrahlung losses (although radiation as a whole remains much less important as a transport channel than heat conduction).

In order to be able to take EC radiation effects consistently into account, the ASTRA transport code [7] has been coupled with the CYTRAN routine [4], which accounts for essential parts of the non-local physics of the EC transport process including wall reflection and which was shown to provide a reasonable approximation to an exact treatment [3].

## 2. Description of the plasma model

### 2.1 Thermal equilibrium and plasma parameters

In order to reduce the effects involved in the electron and ion thermal equilibrium of tokamak plasmas, the source powers are grouped in a unique and fixed term  $P_{source}$ ,

$$\begin{aligned} f_{P_e} P_{source} &= P_{e \rightarrow i} + P_B + P_{EC} + P_{con,e} \\ f_{P_i} P_{source} + P_{e \rightarrow i} &= P_{con,i} \end{aligned} \quad (1)$$

where  $f_{P_{e,i}}$  is the fraction of source power coupled to the electrons and ions ( $f_{P_i} = 1 - f_{P_e}$ ),  $P_B$  is the bremsstrahlung power loss,  $P_{EC}$  is the EC power loss,  $P_{con}$  is the conductive-convective power loss, and  $P_{e \rightarrow i}$  is the electron ion heat exchange due to Coulomb collisions. The electron density being also fixed, the only variable in Eqs. (1) is the temperature.

Throughout this study, the plasma is considered to have a circular plasma cross-section, in order to minimize geometric influences over thermal transport, with major radius  $R = 6.2$  m, minor radius  $a = 2$  m, and with the following values for the magnetic field at the plasma axis,  $B_t = 5.3$  T, and plasma current,  $I_p = 15$  MA. The electron density is taken to be almost flat,  $n_e = n_{e0}(1 - \rho^2)^{0.1}$ , where  $\rho$  is the normalized minor radius and  $n_{e0} = 7 \times 10^{19} \text{ m}^{-3}$ . The total source power follows a Gaussian radial profile with  $P_{source} = 100$  MW. These values are based on non-inductive ITER scenarios [8] and

scaled according to the lower plasma volume of the circular case.

## 2.2 Heat transport model

A very simple heat transport model giving electron temperature profiles consistent with the observed advanced regimes [9,10] is introduced in ASTRA code. The expression for the electron and ion thermal diffusivities is:

$$\chi_{e,i} = \beta_{e,i} \chi_{i,neo} + \alpha_{e,i} [H(\rho - \rho_1) - H(\rho - \rho_2)]$$

where the coefficients  $\beta_e$ ,  $\beta_i$ ,  $\alpha_e$ ,  $\alpha_i$ ,  $\rho_1$  and  $\rho_2$  are adjusted to give consistent electron temperatures profiles, and  $\chi_{i,neo}$  is the neoclassical ion thermal diffusivity.

## 3. Effect of a non-local model for the calculation of the EC radiative transfer on the electron temperature profile

The CYTRAN routine, which is a non-local model for the calculation of the EC radiative power density, is compared to a local model, the Trubnikov's formula  $\left(\frac{dP_{Trub}}{dV}\right)$  locally applied (using the local values of temperature, density and magnetic field for each unit of plasma considered),

$$\frac{dP_{Trub}(\rho)}{dV} = C_T (1 - R_w)^{1/2} a^{-1/2} T_e(\rho)^{5/2} B_{T_0}(\rho)^{5/2} n_e(\rho)^{1/2} \left(1 + \Phi(\varepsilon, T_e)\right)^{1/2}$$

with  $C_T \cong 1.312 \times 10^{-1}$  (when using SI units except for the temperature, which is expressed in keV), and where  $\Phi \cong 18 \frac{\varepsilon}{T_e(\rho)^{1/2}}$ , with  $\varepsilon = a/R$ , accounts for the inhomogeneity of the magnetic field due to toroidal geometry [1]. Such a

simple model is commonly used in some 1D transport studies.

In steady-state conditions and for a very optimistic wall-reflection coefficient of  $R_w = 0.9$  the resulting EC radiative power density ( $dP_{EC}/dV$ ) and electron temperature using one or the other model for the  $dP_{EC}/dV$  calculation are presented in Fig. 1. Although both models give approximately the same total EC power loss ( $P_{EC} \sim 12.2$  MW), when using the local model (Trubnikov's formula) the  $dP_{EC}/dV$  decay is slower and the reversal of the net EC power density in the plasma outer is not reproduced. This qualitative difference enhanced for high wall reflectivities, being extreme for the ideal perfect-wall case ( $R_w \rightarrow 1$ ), where the  $dP_{EC}/dV$  curve using the local formula is zero whilst the non-local model predicts an energy redistribution from the plasma core to the outer plasma, the outer plasma being actually heated.

This energy redistribution due to the transfer of EC radiation is confirmed when the corresponding electron temperatures with  $R_w = 0.9$  in steady-state conditions are analyzed. While the electron temperature resulting of the equilibrium of ASTRA coupled with CYTRAN (the solid curve of the right-side plot) presents three very well distinguished regions,

- a core region with a high and almost flat temperature up to a normalized radius of about 0.3,
- an intermediate region with a strong  $T_e$  gradient going from high values ( $\sim 37$  keV) to low values ( $\sim 6$  keV),
- and the slowly decaying edge region,

the electron temperature when using the local formula presents a very small flat region at the plasma core (up to  $\rho \sim 0.15$ ), having a lower temperature at the intermediate radius  $0.4 \leq \rho \leq 0.7$ . These results are in agreement with those obtained in [11] for D-D burning thermonuclear tokamak plasmas.

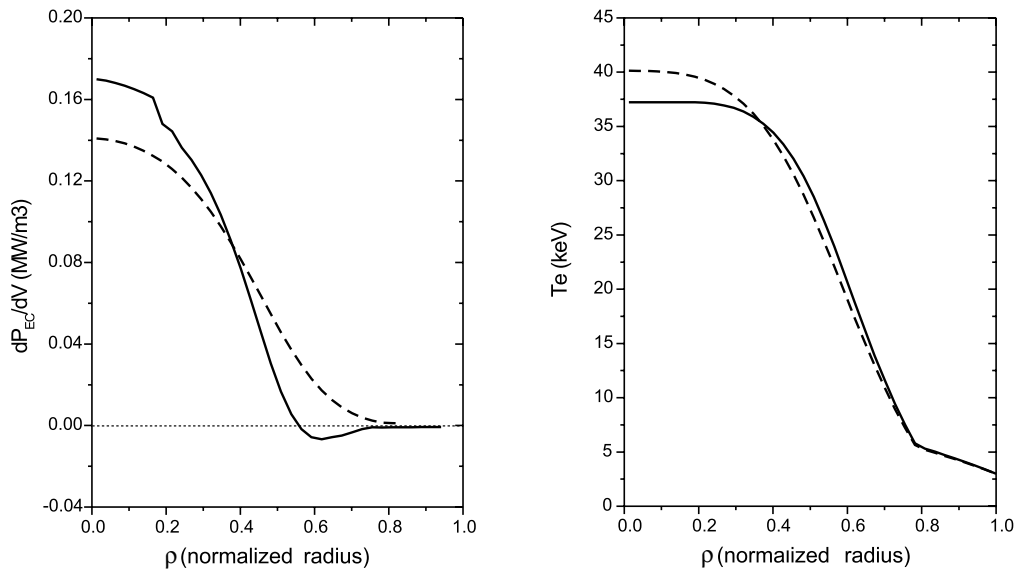


Fig. 1 On the left-side plot, the EC radiative power density calculated using a non-local model (CYTRAN routine), the solid curve, or a local formula, the dashed curve, and on the right-side plot, the corresponding electron temperature in thermal equilibrium.

### 3.1 Sensitivity of the thermal plasma equilibrium to the wall-reflectivity

Using ASTRA code coupled with CYTRAN routine, the effect of the wall-reflectivity on the plasma equilibrium is shown in Fig. 2.

In this figure it is observed that when the wall-reflection coefficient  $R_w$  increases, on the one hand, the EC radiative power density decreases and the reversal of  $dP_{EC}/dV$  at the intermediate region is enlarged, and, on the other hand, the electron temperature increases.

This decrease of  $dP_{EC}/dV$  was already obtained in previous studies [3], where the temperature profile was fixed. In the present case, the enhancement of the radiation self-

absorption when  $R_w$  increases is partially compensated by the observed increase of the temperature, the competition between both effects (self-absorption and emission) being favorable to the first one. This trend is maintained for the entire plasma, and is especially dominant at the intermediate region, where the self-absorption is higher.

Let us analyze in detail the dependence of the electron temperature on  $R_w$ . Being the electron temperature a free variable in our study and the total source power a fixed one, the electron temperature always increases with  $R_w$  in order to obtain a thermal equilibrium in steady-state conditions. In the contrary case, all the terms of power losses, i.e. EC and bremsstrahlung radiative losses and the conductive-convective

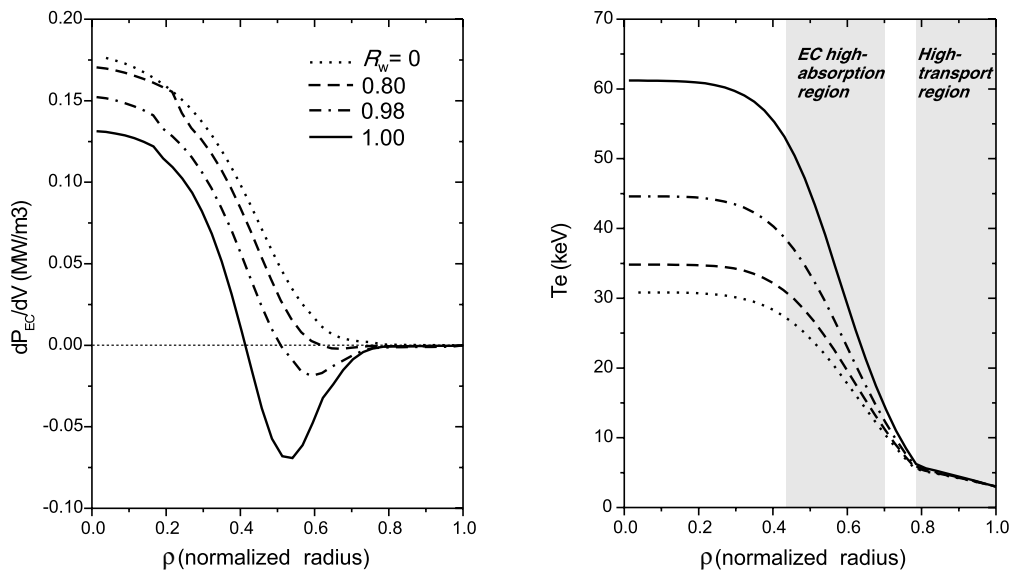


Fig. 2 EC power density and electron temperature in steady-state conditions for different values of the wall-reflection coefficient  $R_w$ .

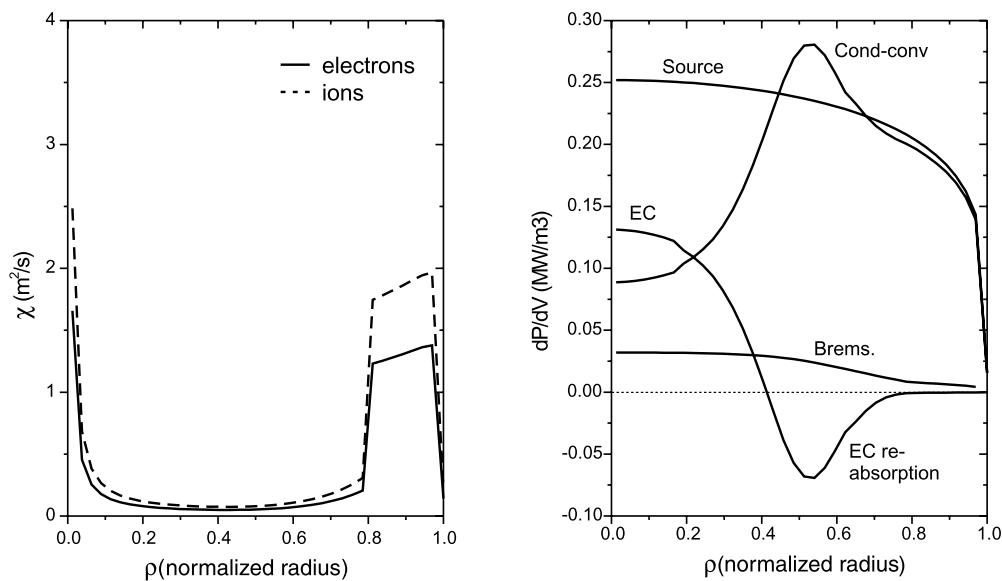


Fig. 3 On the left-side plot, electron and ion diffusivities as a function of the radial coordinate  $\rho$ , and, on the right-side plot, the radial profiles of the source power density, EC and Bremsstrahlung radiative losses, and conductive-convective power loss, for a wall-reflection coefficient of  $R_w = 1$ .

losses, would decrease while maintaining the total source power term. In addition to this, for very high values of  $R_w$ , the resulting profile reversal of  $dP_{EC}/dV$  produces a steeper temperature gradient at the intermediate region, making to increase significantly the electron temperature at the plasma core.

The terms of the thermal plasma power equilibrium in steady-state conditions are evaluated for the ideal limit case  $R_w = 1$ , in order to emphasize the influence of the profile reversal of  $dP_{EC}/dV$ . As it can be shown in Fig. 3, the EC radiative power density represents the dominant term of power losses at the plasma core (for the range  $0 < \rho \lesssim 0.3$ ), being three times higher than bremsstrahlung losses at  $\rho = 0$  (this ratio is still increased for lower values of  $R_w$ ). The profile reversal of  $dP_{EC}/dV$ , localized in the range of  $0.4 \lesssim \rho \lesssim 0.7$ , represents an important heating of up to 30% with respect to the power source.

#### 4. Summary

The non-local effects of the EC radiative transfer on the plasma temperature profile have been evaluated for high-temperature plasmas, by using the ASTRA transport code coupled to a model for the calculation of the EC radiative power density. The energy redistribution produced by the plasma self-absorption of the EC radiation (non-local effect) has a qualitative effect on the plasma temperature. When the total power source and density is fixed, the electron temperature profile increases with the wall-reflection

coefficient, this effect being strongly enhanced for high values of wall-reflectivity, where the reversal of the EC power density at the intermediate region makes to increase the temperature gradient, and consequently the temperature at the plasma centre.

#### References

- [1] B.A. Trubnikov, Reviews of Plasma Physics (M.A. Leontovich, Ed.) Vol. 7, Consultants Bureau, New York, 345 (1979).
- [2] F. Albajar, J. Johner and G. Granata, Nucl. Fusion **41**, 665 (2001).
- [3] F. Albajar, M. Bornatici and F. Engelmann, Nucl. Fusion **42**, 670 (2002).
- [4] S. Tamor, Rep. SAI-023-81-189-LJ/LAPS-72, Science Applications, Inc., La Jolla, CA (1981).
- [5] M. Bornatici, R. Cano, O. De Barbieri and F. Engelmann, Nucl. Fusion **23**, 1153 (1983).
- [6] ITER-FEAT Outline Design Report, ITER EDA Documentation Series No. 19, IAEA, Vienna (2001).
- [7] G. Pereverzev *et al.*, Report IPP 5/42 (1991).
- [8] B.J. Green *et al.*, Plasma Phys. Control. Fusion **45**, 687 (2003).
- [9] JET Team, Nucl. Fusion **39**, 1227 (1999).
- [10] S. Ishida and the JT-60 Team, Nucl. Fusion **39**, 1211 (1999).
- [11] D.C. Baxter and N. Byrne, Nucl. Technology/Fusion Vol. 3, 236 (1982).